Egyptian Geophysical Society
EGS Journal, Vol. 10, No. 1, 73-84 (2012)

IMPACT OF THE GEOLOGIC SETTING ON THE GROUNDWATER OCCURRENCE IN BERKASH AREA – WEST NILE DELTA USING THE GEOELECTRICAL TECHNIQUE

M.S.M. Barseem

Researcher in Desert Research Center
barseem2002@hotmail.com

تأثير الوضع الجيولوجى على تواجد المياه الجوفية فى منطقة برقاش – غرب دلتا النيل باستخدام التقنيات الجيوكهربية

الخلاصة: تواجه مناطق الاستصلاح فى الأراضى الصحراوية العديد من المشاكل الخاصة بالمياه الجوفية من حيث قلة الإنتاجية و زيادة الملوحة. ومنطقة الدراسة هى احدى هذه المناطق و التى تقع شمال الكيلو متر ٣٥ طريق مصر الاسكندريه الصحراوى ويساعد تحديد الوضع الجيولوجى من الصدوع و التغير الجانبى للسحنات الرسوبية على التعامل مع تلك المشكلات و التى تؤثر على الخصائص الهيدرولوجية مثل النفاذية و المسامية. لذلك تم إجراء عدد ١٦ جسه جيوكهربية رأسية لرصد الطبقات الحاملة للمياه الجوفية و تحديد التراكيب الجيولوجية تحت السطحية و مدى تأثيرها على خزان الميوسين ذى الملوحة الأقل نسبيا. كما تم الاستعانة بالمعلومات المتوفرة عن عدد ٢٠ بئراً بالمنطقة.

و لقد اتضح من خلال النتائج أن منطقة الدراسة تتكون من عدد ست طبقات متعاقبة مختلفة فى السمك و المحتوى الصخري ; الأولى هى الطبقة السطحية و التى تتكون من الرمل و تداخلات من الطين و الحصى بسمك يتراوح بين ٣ و ١٢م و مقاومه نوعيه كهربيه تتراوح بين ١٨ و ٣٦٦ اوم.م و تقع فوق الطبقة الثانية ذات السمك الذى يتراوح بين ١١٣ – ١٤٥م و هى طبقة جافة تتكون من الرمل و الحصى و تداخلات من الطين. أما الطبقة الثالثة فهى الحاملة للمياه الجوفية و تتميز باختلافات فى السمك نتيجة التأثر بمجموعه من الصدوع التى يصل عددها إلى ستة مسببة منخفضاً ذا سمك كبير فى منتصف منطقة الدراسة بالإضافة إلى وجود عدسات من الطين فى تلك الطبقة لها تأثير على جودة المياه الجوفية. و لقد وجد من خلال حساب النسبة المئوية لتواجد الطين فى تلك الطبقة أن هذه النسبة تتراوح بين ٥,١ % – ٧١,٦ % و ذلك يعكس الاختلاف الكبير فى قيم الملوحة التى تتراوح بين ٣٢٦ و ١٥٨٧ جزء فى المليون. الطبقة الرابعة ذات مقاومه منخفضة تتراوح بين ٦ – ١٨ أوم.متر عند مواقع الجسات و تتكون من الطين و بسمك يتراوح بين ٩ و ٢٤,٤ م. أما الطبقة الخامسة فهى تتكون من البازلت و يتراوح سمكها من ٣٢,١ إلى ٤٧م و الطبقة الأخيرة تتكون من الرمل الطينى المشبع بالمياه الجوفية و تعتبر الخزان الجوفى الثانى فى منطقة الدراسة حيث المقاومة النوعية لها تتراوح بين ٥ و ٦٩ أوم. متر.

و لتحديد المناطق الأفضل بالنسبة لأولويات استغلال المياه الجوفية و حفر آبار جديدة فقد تم إنشاء خريطة أولويات لمنطقة الدراسة، أتضح من خلالها أن الأجزاء الشمالية و الشرقية هى الأفضل و تقل الأولوية كلما اتجهنا إلى الجزء الجنوبى الغربى و ذلك لقلة سمك خزان الميوسين (الطبقة الأولى الحاملة للمياه الجوفية) و زيادة نسبة الطين و بالتالى زيادة نسبة الملوحة. لذا ينصح الاعتماد على خزان الأوليجوسين (الطبقة الثانية الحاملة للمياه الجوفية) فى الأجزاء الجنوبية الغربية و خاصة عند الجسات أرقام ٢٦، ٣٥ و ٣٦ و ذلك لقلة سمك طبقة البازلت و جودة المياه نسبياً.

ABSTRACT: *Several problems related to groundwater, such as less potentiality and inadequate quality were encountered during the reclamation of the studied area. The present area lies close to km 35, north of the Cairo - Alexandria desert highway with an area of about 16 km^2. The delineation of the subsurface setting helps much in such circumstances. For this purpose, 16 Vertical Electrical Soundings (VES) were carried out. In addition, available data of 20 wells drilled in the area were utilized.*

The interpretation of the VES curves illustrated that the rock succession under the area consists of six layers; a surface layer formed of alluvial deposits with a thickness of up to 12 m and electrical resistivity of 18 - 366 Ohm.m., followed downward with a thick dry zone with a thickness of 113 - 154m and resistivity of 28 - 91 Ohm.m. This second layer is formed of sand , clayey sand and sandy clay. The third layer downward is similar in composition to the second layer but is saturated with water of the Miocene aquifer. It varies in thickness from 25 to 133 m and in resistivity from 24 to 50 Ohm.m. The calculated clay percentage in this area was found to vary from 5.1% to 71.6%, which partly explains the variation in water salinity of this layer from 326 to 1587 ppm. The third layer is underlain by a clayey layer ranging in thickness from 9 to 24 m and in resistivity from 6 to 18 Ohm.m. The fifth member of the succession is formed of basalt with a thickness of 32 - 47 m and resistivity range of 106 - 928 Ohm.m. The last layer downward is formed of sandy clay and clay belonging to the Oligocene aquifer with a resistivity range of 5 - 69 Ohm.m. The interpretation of the geoelectrical data together with the available well data indicted the presence of six normal faults forming a basin in the middle part of the study area.

Based on the depth to water, thickness, clay percentage (water quality) of the shallower aquifer, a priority map was constructed. The map indicated clearly that the promising parts of the area, as to the drilling of water wells, are the eastern and northern parts. In the southern and western parts, the deeper aquifer (Oligocene) lying under the basalt sheet may be utilized for relatively better water quality. VES stations 26, 35 and 36 are considered to be the best sites for the drilling of water wells reaching to the Oligocene aquifer in these part of the area.

INTRODUCTION

Reclamation of the desert areas lying to the west of the Nile Delta has received special attention from the government and different investment authorities for agricultural development. One of these areas is Berkash area, north west of Cairo. Many farm owners faced serious problems concerning groundwater potentiality and degradation of quality. Several factors play significant role in the occurrence and supply of groundwater such as sedimentary succession, the geologic structure and lateral facies change. In the present study the geoelectrical resistivity soundings and the lithological information of wells were used to delineate the following:

a. The sedimentary succession and its vertical and lateral facies changes.

b. The extension of water-bearing formation.

c. The impact of geological structures on the groundwater occurrence and quality.

d. The distribution of the basaltic sheet and its contribution to the occurrence and flow of groundwater.

More emphasis in the application of the VES technique was made in that part of the area free of water wells.

The study area (Fig. 1) is bounded by latitudes 30° 57' 00" to 31° 1' 48" N and longitudes 30° 4' 48" to 30° 9' 00" E. It lies North of km. 35 (Cairo – Alexandria Desert Highway) with an area of about 16 km^2.

HISTORICAL STUDIES

The study area has been subjected to many works, aiming at delineating the geomorphological, geological and hydrological setting. These works were made by Shata (1961), Shata and El Fayoumy (1967), Said, (1962), Omara, Sanad (1975), Sand (1973), Attia (1975), Abd El Baki (1983), CONOCO (1987), Abd El Rahman (1996), Ezz El deen (1999) and Ahmed (2002).

Geomorphologically, the study area lies southwest of the Nile Delta at Berkash (Fig 2). The region within which the area is located characterized by a slightly undulating land surface, which slopes generally towards the Nile Delta. It is divided into two main geomorphologic units; the alluvial plains and the structural plain. The alluvial plains are differentiated into the young and the old alluvial plains. The young alluvial plain occupies the cultivated flat areas west of the Nile Delta and is composed of silt, clay and sand. The old alluvial plain lies to the south of the young alluvial plain and it is characterized by slight undulation with several low lying hills and dominated by sand and gravel. The structural plain occupies the wide area to the south of the old alluvial plain. It is an extensive pavement plain which consists of a number of alternating ridges.

Geologically, the area under study is lithologically covered by sedimentary rocks belonging to the Holocene and Pleistocene (Fig. 3).

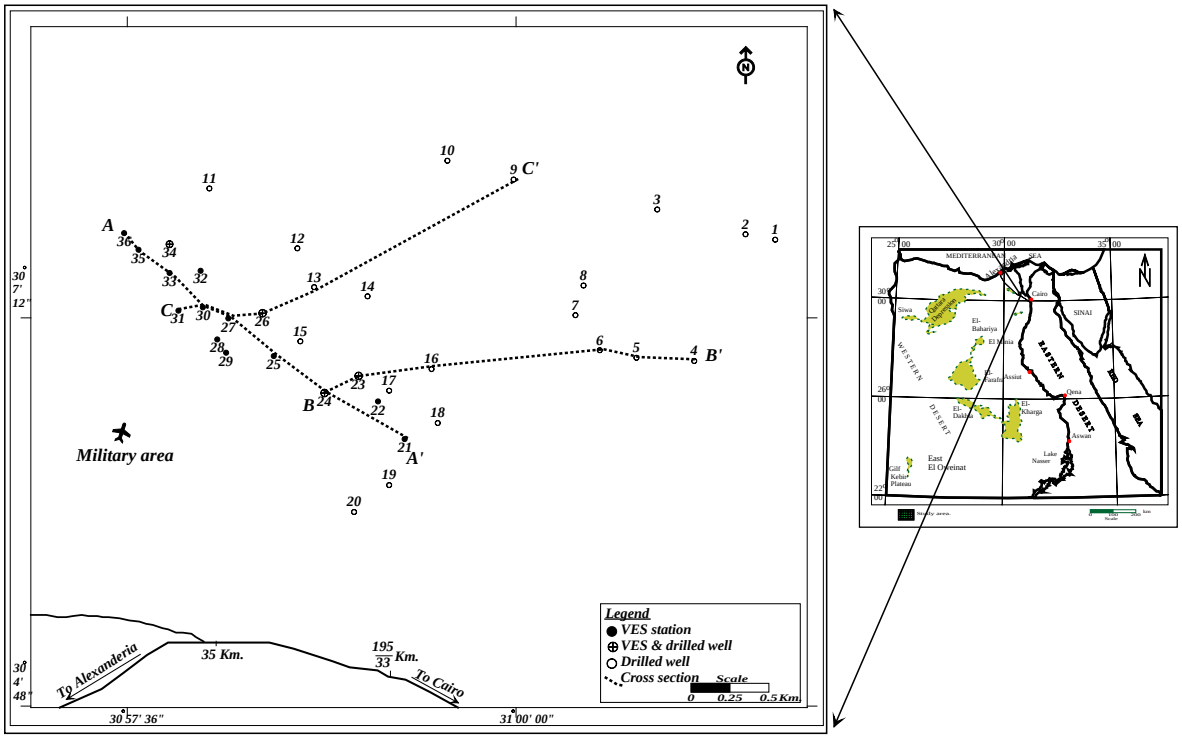

Fig. (1): Location map of the study area and sites of geophysical measurements.

According to, Abd El Baki (1983), El Ghazawi, (1982) and El Ghazawi and Atwa (1994), the area is composed of aeolian sand and gravel with occasional clay interbeds. These deposits are underlain by the Lower Miocene sediments (Moghra Formation) which is composed of sand and gravel with clay intercalations. The Oligocene basalt underlies the Lower Miocene deposits and overlies the Oligocene sediments represented by clay and sand interbeds. The detection of a basaltic sheet at different levels reflects the effect of structures on the geologic succession and on the groundwater occurrence. The Eocene deposits underlie the Oligocene deposits. They are represented by chalky, clayey and sandy limestone grading into marls and clay as well as sandy marls and clays (Said 1962, Shata 1962 and El Shazly, et al., 1975).

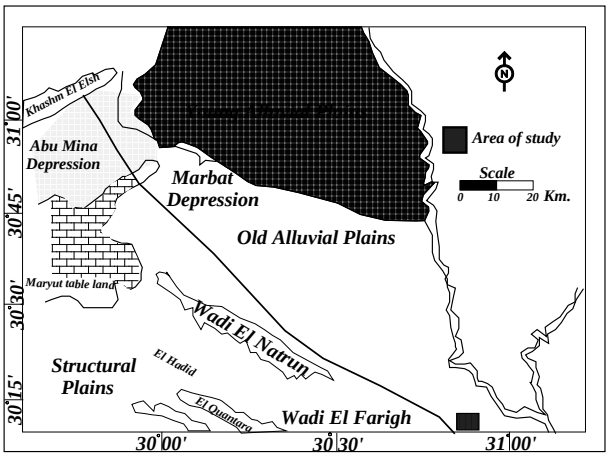

Fig. (2): Geomorphology map of the study area (After Abd El Baki, 1983).

The southern part of the Nile Delta comprising the study area is structurally affected by two normal faults systems. The first is NE – SW (Aqaba system) as those faults bounding Wadi El Farigh from the north and the south. The other fault system belongs to the NW – SE (Clysmic).

Hydrogeologically, the investigated area is characterized by an arid to semi arid climate with hot summer and mild rainy winter. The water-bearing formation in the southwestern part of the Nile Delta belongs to the Pleistocene, Lower Miocene (Moghra Formation) and Oligocene aquifers. The last two aquifers are separated by the Oligocene basalt sheet (Abd El Rahman, 1996).

According to Ahmed (2002) the Pleistocene aquifer is directly recharged from El Mansouria canal and its different branches as well as surface seepage from the cultivated lands. The depth to water varies from 5 to 12m. The total dissolved solids (TDS) range between 335 and 1056 ppm.. The depth to water in the Lower Miocene aquifer varies from 56 to 142 m. The saturated thickness is controlled by the structural conditions prevailing in the area of study where, it ranges between 27 and 169 m. The Oligocene reservoir is a confined aquifer due to the presence of the basaltic sheet. The depth to water reaches 130 m from the ground surface. The water of this aquifer is slightly fresh (1056 ppm). The recharge of this aquifer may be due to the hydraulic connection with the overlying fractured Miocene aquifer.

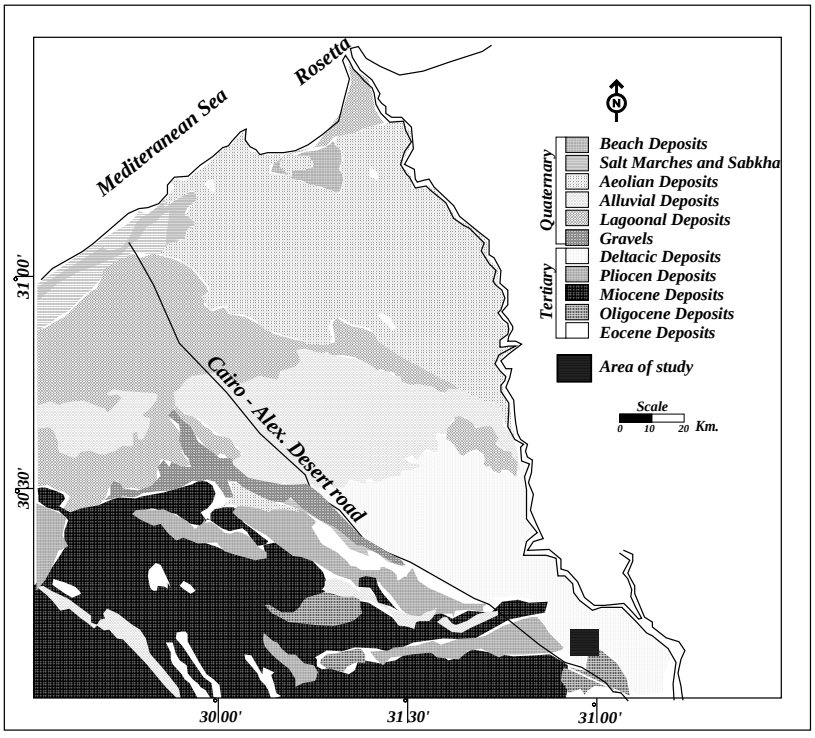

Fig. (3): Geologic map of the study area (After CONOCO, 1987).

FIELD MEASUREMENTS

A total of 16 Vertical Electrical Soundings were carried out in the area of study. Some of the VES stations were conducted near by the drilled wells in order to obtain parametric measurements. Such measurements are considered a basis for the quantitative interpretation of the measured field curves. Also the available data of 20 drilled wells were used. These data comprised litholigical description, thickness of the successive layers and depth to water. Figure (4) shows examples of the field sounding curves. Figure (5) shows an example of the well log with litholigical description.

The Schlumberger techniques configuration was used in the VES measurements. At each VES station, the apparent resistivity (ρ_a) was measured for progressively increased current electrode spacing, represented by the value of AB.

In all the measured soundings the current electrodes half spacing (AB/2) was started with one meter and ended with 2000m. This was the maximum spacing which could be reached in the area due to some military security restrictions. However, it was enough to reach the formation beneath the Tertiary basalt. The Terrameter SAS 1000 resistivity meter was used to measure the resistance ($\Delta V/I$) with high accuracy.

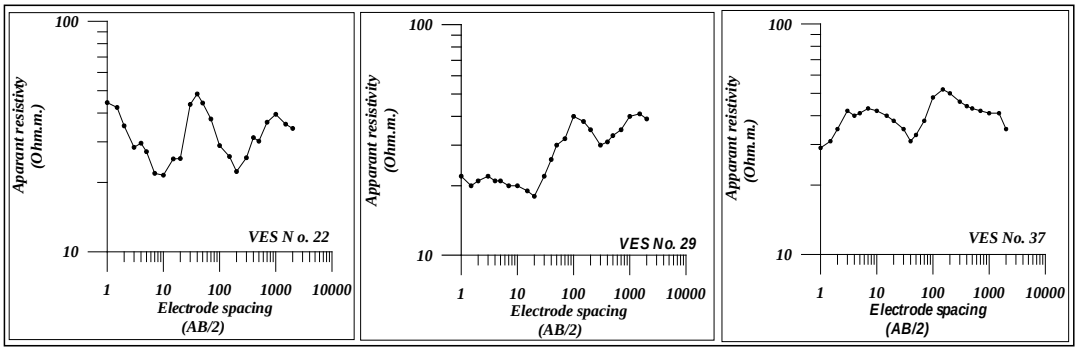

Fig. (4): Examples of the resistivity sounding curves.

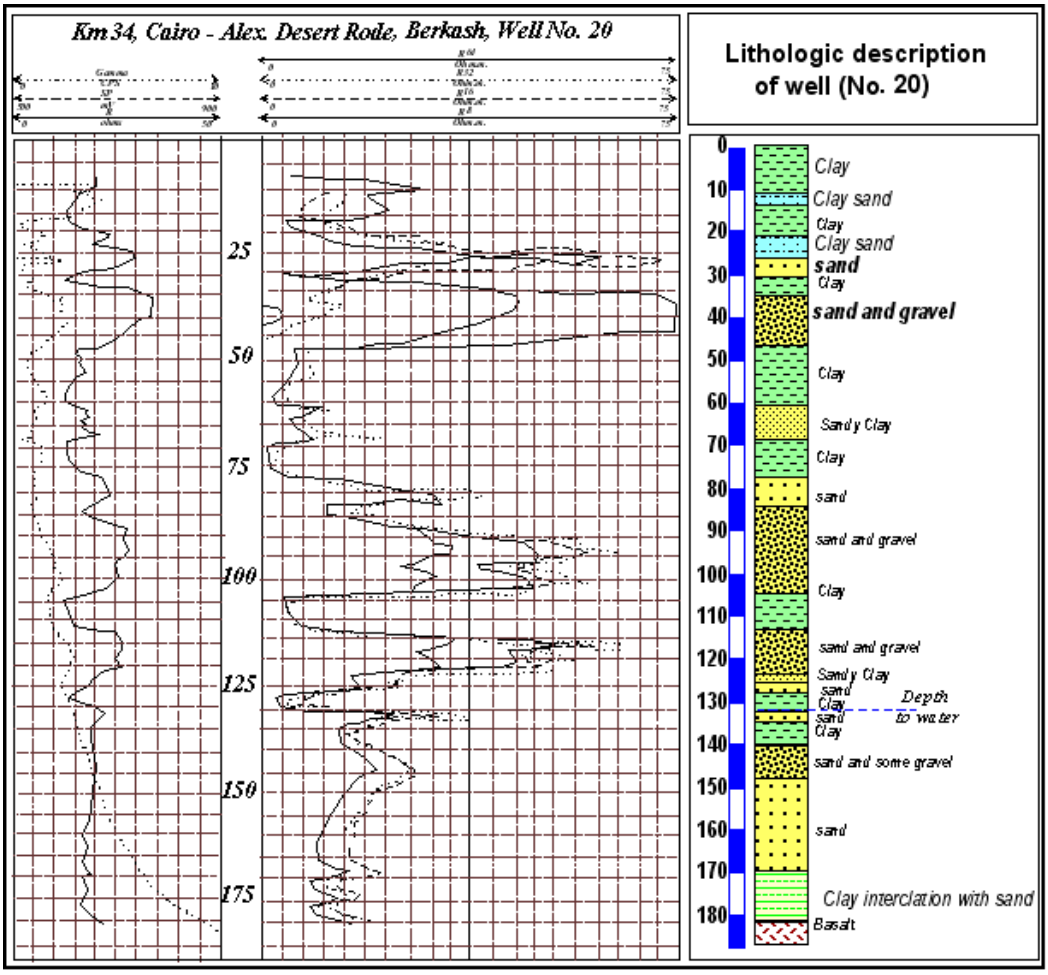

Fig. (5): Well log and lithologic description of well No. 20.

The topographic map scale (1 :25,000) and the Global Positioning System (GPS) were used to determine the accurate locations and ground elevations of the sites of both the geoelectrical sounding and drilled wells (Table 1).

Table (1) Ground elevations of the drilled wells and VES stations.

Drilled well No.	Elevation (m.)	VES No.	Elevation (m.)
1	64	21	135
2	64	22	144
3	57	*23	152
4	105	*24	158
5	132	25	158
6	138	* 26	159
7	130	27	160
8	105	28	160
9	100	29	160
10	109	30	156
11	127	31	158
12	161	32	158
13	137	33	153
14	151	*34	162
15	152	35	167
16	147	36	166
17	153	* VES & Drilled well	
18	148		
19	165		
20	133		

RESULTS AND DISCUSSION

The field data of the Soundings have been interpreted qualitatively and quantitatively to delineate the subsurface sequence of the geoelectrical layers in the area of study.

Concerning the qualitative interpretation: According to the obtained VES curves, the resistivity values along the first and second cycles (AB/2 = 1 to 100) represent surface and near surface variations. They reflect heterogeneity characterizing the surface layers. This heterogeneity is due to the clay beds intercalating the sand and gravel deposits. In going downwards on the field curves (third cycle at AB/2 > 100m.) show nearly the same type is shown which reflects homogeneity and continuous aerial extension of the deeper layers. At this part the field type KHQ dominates.

This curve type indicates the last detected geoelectrical layer that has the least resistivity value, corresponding to the water-bearing formation. There are some variations in the field curves due to the variations in the depth of penetration of the water-bearing formation and the presence of clay intercalations . The curves of the H- type are mostly due to the effect of the basalt sheet which is characterized by relatively higher apparent resistivity.

The Quantitative interpretation: Provides the true resistivities, depths and thicknesses of the geoelectrical layers. These parameters become the main source of information which can delineate the subsurface geologic succession, structures and water-bearing formation, then presented in the form cross section and different types of maps. The VES curves were interpreted quantitatively by constructing a model for each curve, using the computer program RESIST, (Van Der Velpen 1988). It is a non automatic iteration method in which the measured field data are compared with data calculated from an assumed model. The models were prepared with the aid of the collected data of some wells near the VES stations. Figure (6) shows the interpretation of VES No.34 beside well. In order to reach an optimum correlation between the geoelectrical layers and the geologic units, some successive geoelectrical layers have been grouped together in one layer. The resistivity of such layer is expressed in terms of the average transverse resistivity (ρ_t) (Abd El Rahman 1996), calculated as follows:

$$\rho_t = \sum(\rho_i * h_i) / \sum h_i \quad \text{.....i = 1 to n}$$

Where;
ρ_i is the resistivity of the **i**th layer,
h_i is its thickness,
n is the number of layers

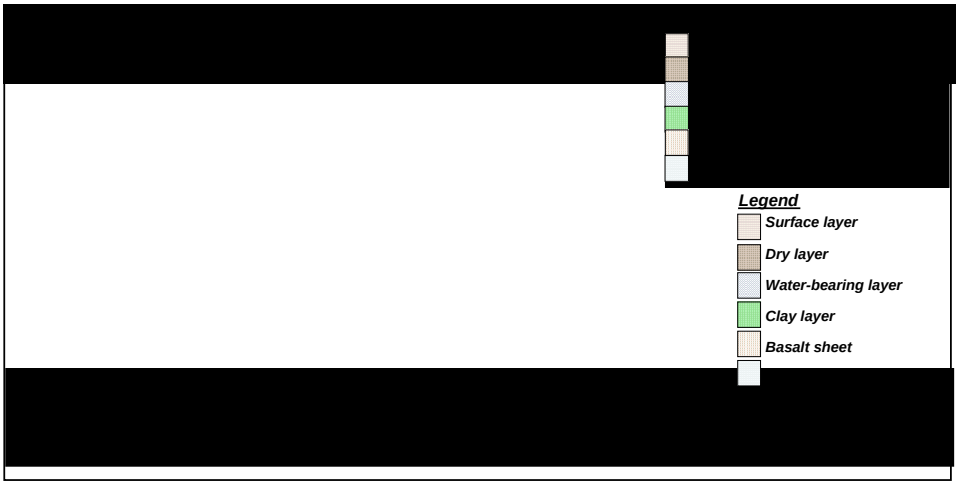

Fig. (6): The interpretation of VES No. 34.

The result of the quantitative interpretation of the 16 VES curves are listed in table (2). From these results, three geoelectrical cross sections (Fig.1) were constructed (A-A`, B-B` and C-C') covering the study area (Figs. 7, 8 and 9). These cross sections together with well data show that the subsurface of the area is vertically distinguished into six main geoelectrical layers, illustrating the geoelectrical sequences, lateral and vertical variation of the different layers and the subsurface structures. The main common features and observations are the following:

1. The first layer is the surface zone which extends from the surface downwards to a depth varying from 2.5 m at VES No 34 to 20 m at VES No. 22 and has a resistivity ranging from 18 Ohm.m at VES No. 30 to 366 Ohm.m at VES No. 24. The wide range of resistivity may be due to change in lithology from sand to sandy clay to clay.
2. The second layer consists of several layers grouped together in one layer. It has a thickness ranging from 113 m at VES No. 22 to 154 m at VES No. 35. This layer exhibits resistivity varying between 28 Ohm.m at VES No. 21 and 91 Ohm.m at VES No. 24, which corresponds to dry sand with clay intercalation and gravel.
3. The third layer is nearly similar to the second layer in lithological composition, where it consists of sand and gravel. It represents the water-bearing zone. The resistivity of this layer ranges from 24 Ohm.m at VES No.31 to 50 Ohm.m at VES No. 22 and thickness from 25 m at VES No 24 to 133 m at well No. 14. The large variation in thickness may be due to the effect of faulting.
4. The fourth layer consists of clay underlying the water-bearing layer. It has a thickness ranging from 9 m at VES No. 30 to 24.4 m at VES No. 23 and exhibits low resistivity ranging from 6 Ohm.m at VES No. 31 to 18 Ohm.m at VES No. 29 Ohm.m..
5. The fifth layer has nearly a uniform thickness ranging from 32 m. at VES No. 31 to 47 m at VES No. 27. This zone has resistivity varying between 106 Ohm.m at VES No. 31 and 928 Ohm.m at VES No. 24.

Table (2): Results of interpretation of the VES curves.

VES No	Surface zone		Dry zone		Water bearing zone		Clay zone		Basalt sheet zone		sandy clay zone
	ρ	h	ρ	h	ρ	h	ρ	h	ρ	h	ρ
21	28.56	3.80	27.95	121.00	45.60	47.60	8.20	9.90	202.10	40.30	32.70
22	20.31	20.10	53.92	113.00	50.30	40.70	8.80	9.10	166.90	32.80	17.40
*23	105.20	4.40	76.53	123.00	16.40	58.20	9.60	24.40	200.40	39.00	68.50
*24	366.08	7.60	90.86	128.90	41.30	24.80	13.80	9.70	927.80	30.90	10.60
25	27.67	3.80	30.98	137.60	49.30	55.00	8.80	9.30	202.90	36.80	23.70
*26	27.36	8.70	45.71	144.30	35.60	47.00	12.60	8.20	145.60	37.20	27.70
27	80.03	12.30	60.56	139.30	32.00	53.20	11.60	9.50	482.50	47.00	7.20
28	22.33	5.40	42.61	146.10	20.10	55.00	8.90	10.90	577.20	41.40	26.60
29	18.13	4.20	44.91	131.90	30.50	54.70	17.60	10.00	375.60	37.30	9.00
30	17.88	7.20	30.73	141.30	37.50	48.40	7.50	9.00	187.10	38.00	31.00
31	19.70	7.30	35.11	141.10	23.70	44.00	5.70	10.50	105.50	32.10	16.50
32	45.08	8.70	61.29	135.40	54.80	54.80	9.00	9.00	155.30	36.10	19.90
33	37.25	4.10	72.38	135.40	44.50	49.80	7.80	8.10	217.00	43.60	4.70
*34	35.92	2.50	41.44	145.4	47.40	58.90	7.40	20.00	770.70	42.70	21.90
35	56.99	2.70	65.71	154.60	49.50	54.50	7.00	10.00	279.80	39.30	35.30
36	44.93	2.90	57.19	152.80	31.20	52.90	4.30	11.10	237.90	34.20	33.40

ρ = True resistivity (Ohm.m.) h =Thickness (m.) * VES beside well

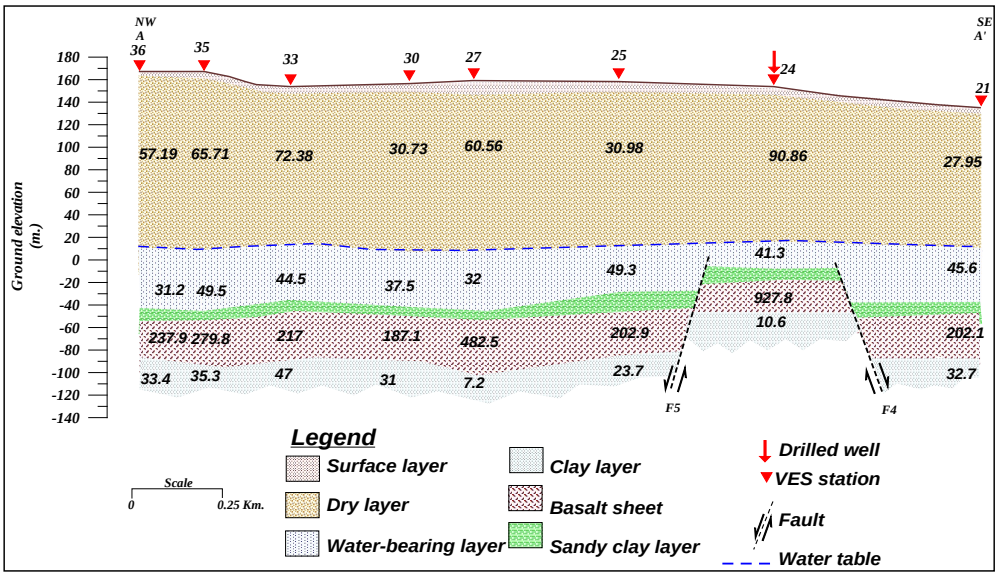

Fig. (7): Geoelectrical cross sections AA'.

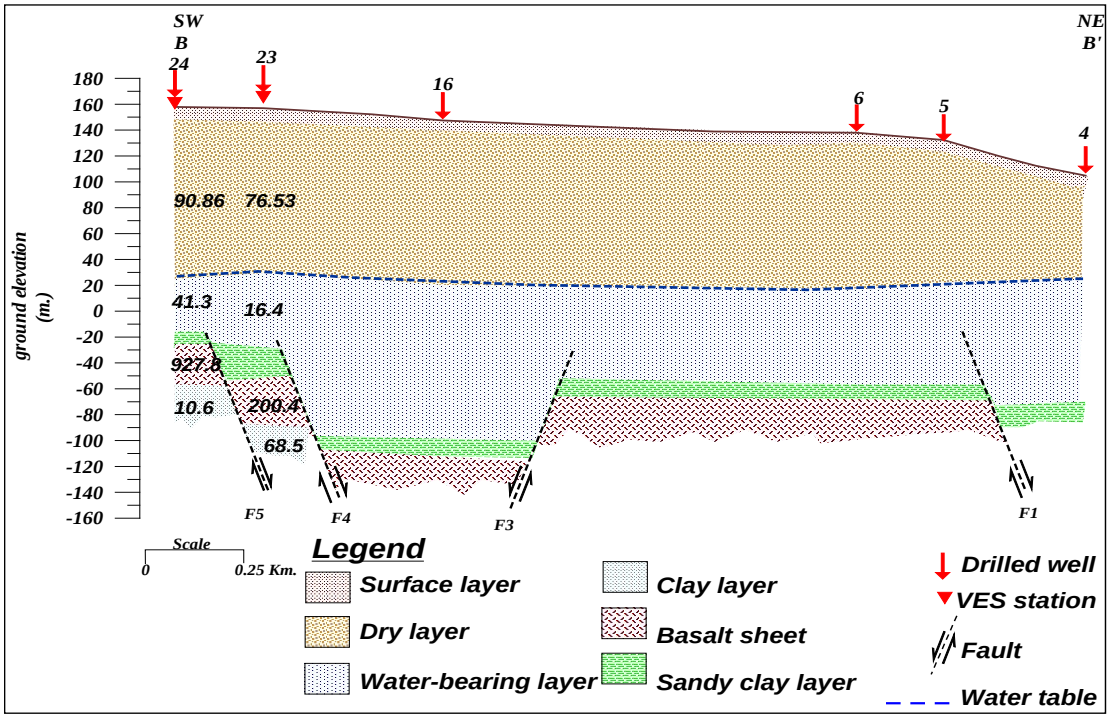

Fig. (8): Hydrogeoelectrical cross sections BB'.

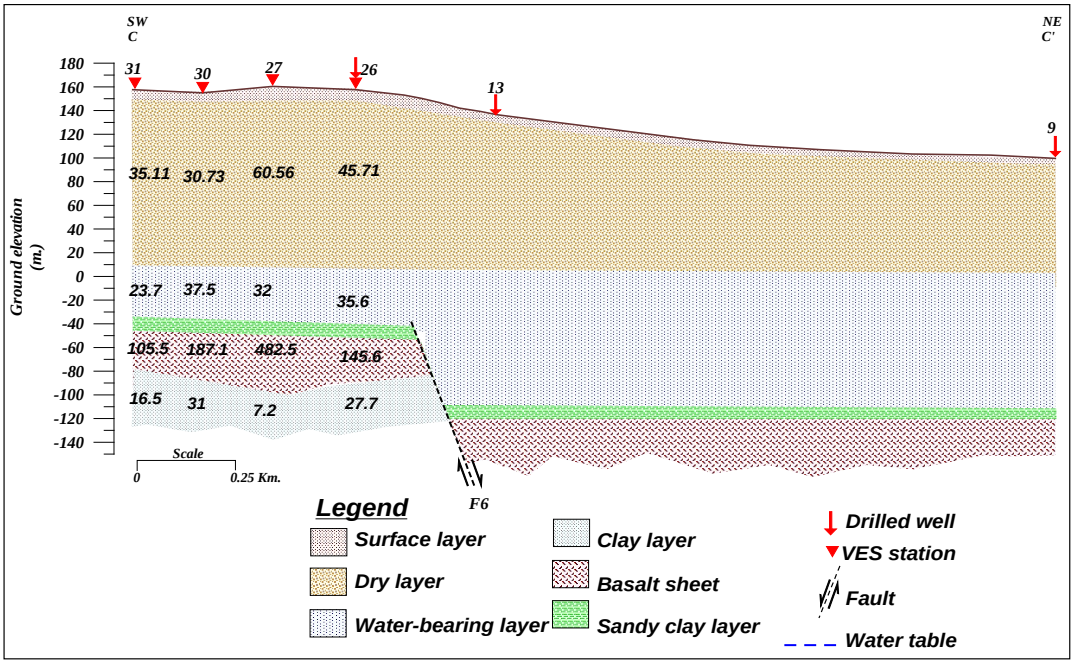

Fig. (9): Hydrogeoelectrical cross sections CC'.

It corresponds to the Oligocene basaltic sheet which extends under the study area with gently undulated upper surface. The relatively low resistivity of the basalt at some VES stations is attributed to the weathered and /or fissured nature of this sheet, in addition to the possibility of water saturation.

6. The last detected geoelectrical layer has a resistivity ranging from 5 Ohm.m at VES No. 33 to 69 Ohm.m at VES No. 23. It consists of Oligocene sandy clay and clayey sand. It represents the second water-bearing layer. The base of this layer was not reached as it represents the last member of the geoelectrical succession.
7. The lithologic succession is affected by normal faults. These faults affect the thickness of the water-bearing formation above the basaltic sheet.

HYDROGEOLOGICAL SETTING

The water-bearing formations in the study area were classified according to the geological and hydrogeological information from the drilled wells and the geophysical results into two main aquifers. The first aquifer is the Lower Miocene aquifer known as the Moghra Formation. It is composed of sand, sandstone and interbeds. These sediments are overlain by the Quaternary deposits e.g. aeolian sand and or nilotic sediments and are underlain by the Oligocene basaltic sheet (Abu Zaabal Formation). This aquifer is considered to exist under semiconfined conditions. The second one is the Oligocene aquifer which underlies the basalt sheet and consists of sand, clayey sand and clay. It is found to exist under confined to semiconfined conditions. The geoelectrical cross sections revealed that the two aquifers are hydraulically connected as a result of faulting.

The data of the depth to water measured in the wells and that obtained from the VES interpretation have been used to construct a contour map for the depth to water (Fig. 10). This map shows that the maximum depth to water is 157.3 m at VES No. 35 in the northwestern direction and the minimum value is 24 m at VES No. 1 in the northeastern direction. Generally, the depth to water slopes from east to west. The direction of the groundwater flow can be detected from the water level contour map (Fig. 11). From this map, it is clear that the groundwater flow is generally from east to west and northwest direction, the variation in flow patterns is mainly attributed to the lithological variations and the structural elements prevailing the study area. Thus, it becomes necessary to illustrate these variations in details as follows:

- ***Lithologic variation***:

The clay lenses and clayey sand as impervious layers, thus affecting hydraulic parameters such as transmissivity, hydraulic conductivity and yield. The estimation of sand and clay percentage within the water-bearing layer at both the drilled wells and VES stations becomes more useful according to Abd El Rahman, (1996). The sand percentage of the water-bearing layer has been estimated by making use of true resistivity (ρ_t) of the water-bearing calculated at VES stations adjacent to boreholes. The maximum true resistivity (ρ_{tm}) with the value of 47.4 Ohm.m at VES No. 5 adjacent to well was found to correspond to a lithologic succession consisting of 82% sand and 8% clay (calculated in terms of sand and clay layers thickness). In order to estimate the sand percentage at other VES stations, the product ρ_t / P_{tm} of water bearing at each VES station was multiplied by 82 instead of 100, i.e.

$$Sand\ percent = \rho_t / \rho_{tm} * 82$$

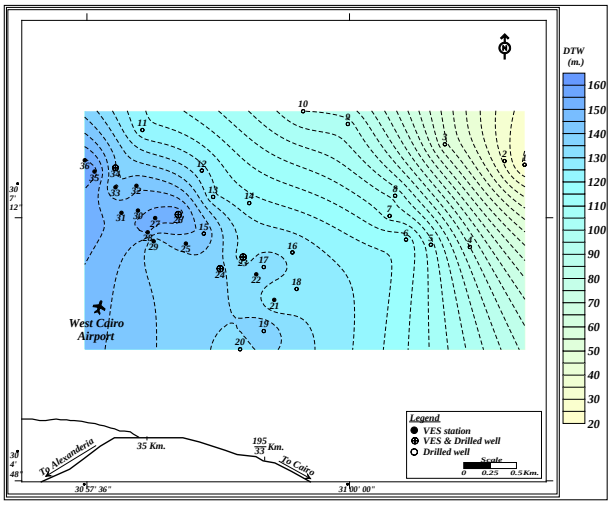

Fig. (10): Depth to water contour map.

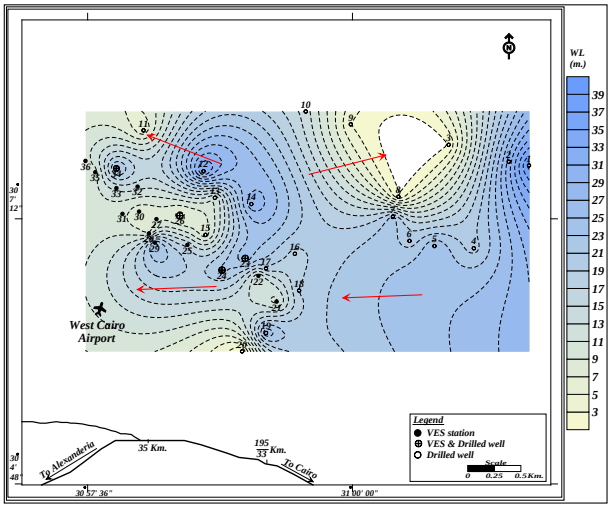

Fig. (11): Water level contour map.

The clay percentage in the water-bearing layer can be calculated by subtracting from 100. The maximum clay percentage was found to be 71.6 % at VES No. 23 whereas, the minimum clay percentage was found to be 5.1 % at well No. 8. These data are represented by the histogram of Fig. 12. These data were used to construct the contour map of Fig. 13 to exhibit the effect of clay lenses on the water-bearing layer. From this map, it is clear that the western parts of the study area represent the higher clay content in the water-bearing formation.

in

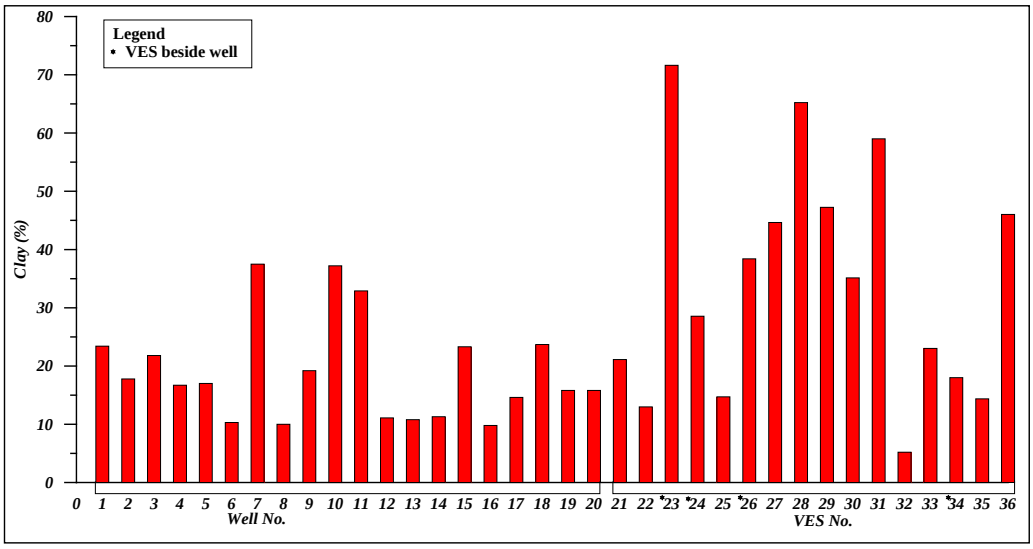

Fig. (12): Histogram of the clay percentage in the water bearing zone

This is confirmed by the values of water salinity obtained by Ahmed (2002) for the Lower Miocene aquifer. The salinity of the Miocene aquifer increases from east to west from 326.4 ppm at well No. 1 to 1587 ppm at drilled well No. 19. The low salinity of groundwater of the Lower Miocene aquifer reflects direct recharge from the great basin underlying Rosetta branch of the Nile through fault.

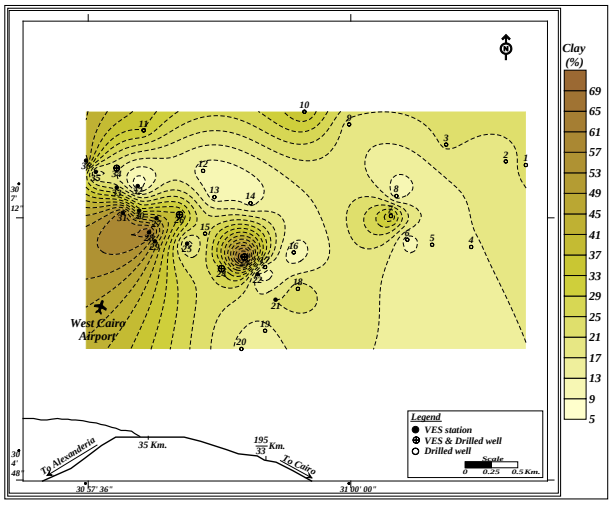

Fig. (13): Contour map of the clay percentage.

- ***Inferred Structure:***

The other parameter that affects the hydrological condition in the study area is the geologic structure induced by faulting. The delineation of faults affecting the basalt sheet certainly helps in recognizing the hydrogeologic variations of the water-bearing layers. The basaltic sheet has maximum resistivity values of 771 Ohm.m at VES No. 34 and minimum resistivity value of (106 Ohm.m at VES No. 31 (Table No. 2). The variation in the resistivity value is mainly attributed to the weathered and fractured nature of the basaltic sheet addition to the possibility that it is partially saturated with water. The variation in depth to basalt from ground elevation has been exhibited as a contour map (Fig. 14).

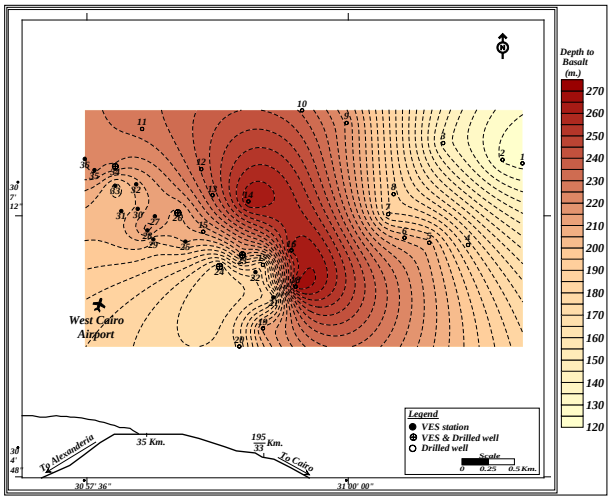

Fig. (14): The clay percentage contour map.

This map shows that the depth to the surface of basalt sheet increases from both the northeast and southwest directions to the central parts of the study area. The maximum depth to basalt sheet is 268 m at drilled well No. 18 while the minimum value is 124 m at well No. 2. The abrupt change in the depth to surface of the basalt sheet is due to faulting. The level contour map of the basalt sheet (Fig. 15) helped in deducing some of these faults. It is clear from this map that the central part of the study area lies at a higher level than the surrounding parts. From the basalt level contour map and the constructed geoelectrical cross sections some faults can be detected as shown in (Fig. 16). From this map, it is clear that six normal faults affect the study area, striking NW – SE (F4, F5, F3 and F6), NE –

SW (F2 and F1) directions. The throw of the faults F4, F5, and F6 is towards the east while that of the faults F2 and F3 is towards the west. The last minor fault F1 throws towards the south direction. These faults affect the thickness of the water-bearing layer above the basaltic sheet. The isopach contour map of the water-bearing formation (Fig. 17) shows the variation in thickness. From this map it is clear that the maximum thickness (133 m) is at well No. 14 and the minimum thickness (24 m) is at VES station No. 24. This map shows a uniform thickness decreasing in the western direction.

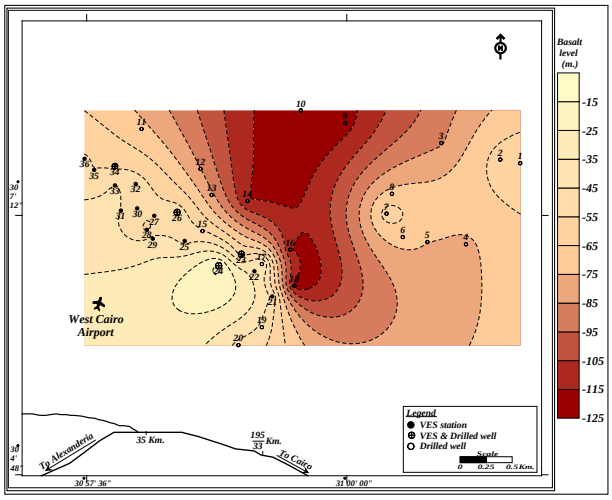

Fig. (15): Level contour map of the basalt sheet.

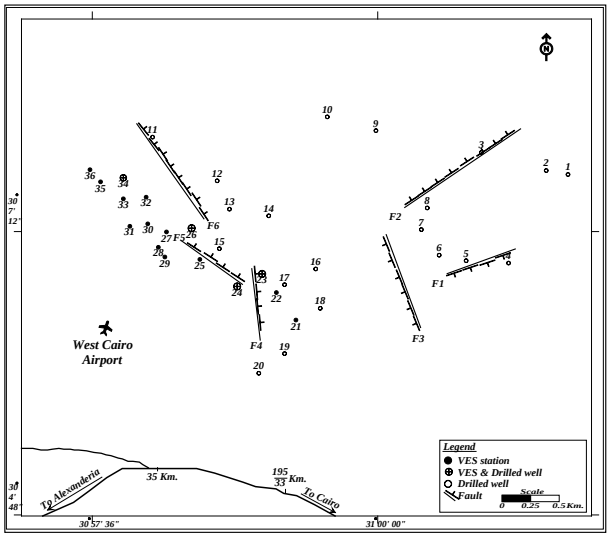

Fig. (16): Inferred faults for the study area

According to the above discussion, sites where the water-bearing layer has a lower clay percent (less salinity), higher thickness and less depth to water would be recommended for the drilling of new water wells, for which the weighting factors of these parameters are 50%, 30% and 20%, respectively . For the construction of the priority map of the water-bearing zone , the clay percent, thickness and depth to water have been categorized into four categories respectively (Table 3). From the priority map of the water-bearing layer (Fig. 18), it could be concluded that the most promising area for drilling wells tapping this layer is located at the eastern parts. The less priority exists in the southwestern part.

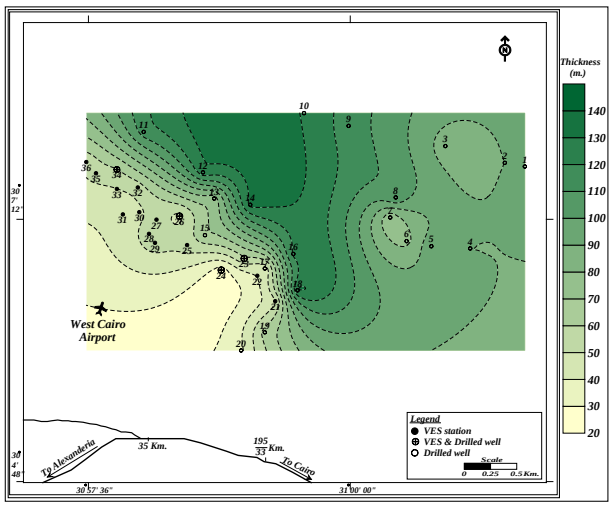

Fig. (17): Isopach map contour map of thewater-bearing layer

Table (3): Clay percent, thickness and depth category ranges for the water-bearing layer.

Category	Clay percent (%)	Thickness (m)	Depth to water (m)
1	< 5	> 100	< 100
2	6 - 20	60 - 101	101 - 120
3	21 - 60	20 - 60	121 - 140
4	> 60	< 21	> 140

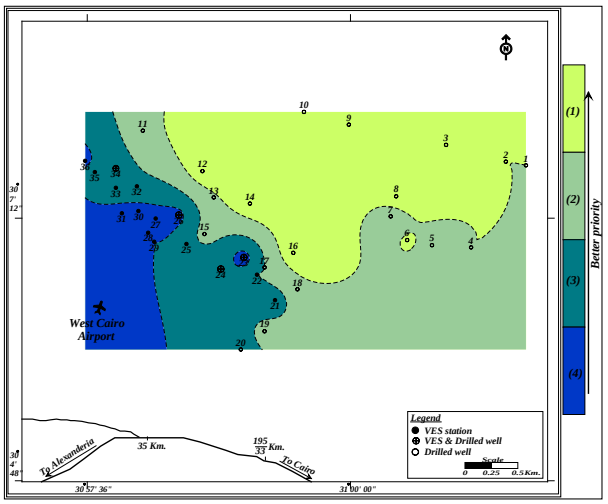

Fig. (18): Priority map for groundwater exploitation along the water bearing zone

CONCLUSIONS

From the results of the study, with the purpose of delineating the impact of geoelectrical setting on the ground water occurrence in the study area, the following can be concluded:

1. The geological succession consists of six layers as derived from the interpretation of the sounding curves VES stations and drilled wells information . The first layer consists of intercalations of gravel, sand, clayey sand and sandy clay. The second layer consists of a thick dry zone formed of sand and clay intercalations overlying third layer which is composed of sand and represents the water-bearing layer. The fourth layer represents the end of the above layer which consists of clay. The fifth member of the succession consists of the Oligocene basalt. The last layer consists of water-bearing Oligocene, formed of sandy clay.
2. The depth to water measured from the ground surface at the sites of sounding stations and wells ranges from 24 to 157.3 m. The water level lies at about 39 m above sea level.
3. The thickness of the water-bearing layer ranges from 24 to133 m which generally decreases in the western direction.
4. The presence of clay lenses and sandy clay affect the hydraulic parameters (transmissivity, hydraulic conductivity and yield) of the water-bearing layer. The calculated clay percentage at each VES station and well shows that the western parts of the study area have the higher clay content in the water-bearing formation and, so the high salinity.
5. The Oligocene basaltic sheet is affected by six normal faults that make large basin in the central part of the study area.

RECOMMENDATION

According to the results of the above study, the following recommendation can be made:

1. The priority map for the water-bearing layer of the Miocene aquifer shows that the most promising area for drilling water wells is located in the northern part.
2. In the part of the area having less in priority of the Miocene aquifer, it is recommended to penetrate the hard basaltic sheet to reach the Oligocene water-bearing layer although of less quality and expected less discharge. The relatively best sites for well drilling to reach this layer are at VES station (26, 35 and 36).
3. Well logging is important to define the accurate boundaries of the sedimentary succession and to put the suitable design of the wells to be drilled.
4. Pumping test is necessary to estimate the hydraulic parameters of the saturated zones.
5. It is strongly recommended that prior to any drilling activity, a geophysical study should be conducted at the desired sites.

REFERENCES

Abd El Baki, A.A. (1983): "Hydrogeological and hydrochemical studies on the area west of Rosetta branch and south El Nasser Canal". Ph. D. Thesis, Fac. Sci; Ain Shams Univ. Cairo, Egypt, 156p.

Abd El Rahman A. A., (1996): " Geophysical study on the groundwater conditions in the area southwest of the Nile Delta between Abu Roash and El Khatatba road" M.Sc. Thesis, Fac. SCi., Ain Shams Univ., Egypt, 122p.

Ahmed, K. A., (2002): " Hydrogeological studies on the groundwater aquifers in the northwest Cairo", Ph. D. Thesis, Fac. Sci. Al Azhar Univ. 113P.

Attia, S. H., (1975): " Pedology and soil genesis of Quaternary deposits in the region west of the Nile Delta (North east of Wadi El Natrun)" Ph.D. Thesis, Fac. Sci., Ain shams Univ., 228p.

CONOCO (1987): Geological map of Egypt, NF 36 NW El Sad El Ali. Scale 1:500000. The Egyptian General Petroleum Corporation. Conoco Coral.

El Ghazawi, M.M. (1982): "Geological studies of the Quaternary – Neogene aquifers in the area northwest Nile Delta" M.Sc. Thesis, Fac. Sci., Al Azhar Univ; Cairo, Egypt, 170 p.

El Ghazawy, M. M. and Attwa, S. M., (1994): "Contribution of some structural elements to the groundwater conditions in the south western portion of the Nile Delta", Egypt J. Geol., 38- , p.649 - 667.

El Shazly, E. M., Abd El Hady, M. A., El Ghawby M. A., El Kassas, I. A., Khawasik, S. M., El Shazly, M. M. and Sand, S., (1975) :" Geologic interpretation of landsat satellite images for West Nile Delta area, Remote sensing Center, Academy of Scientific Research and Technology, Cairo, Egypt, p38.

Ezz El Deen, H. M. M., (1999): Implication of the subsurface structures on the groundwater aquifers in the area between km 38 and km 46, Cairo – Alexandria desert road, Egypt" E.G.S. Proc. of the 17th ann. Meet., March, 1999, 99. 111 – 130.

Omara, S. M., and Sanad, S. (1975): " Rock stratigraphy and structural features of the area between Wadi El Natrun and Moghra Depression, Western Desert, Egypt" Geol. J., Bl 6, Hannover, p. 45 - 73.

Said , R., (1962): " **Geology of Egypt**, ElSevier, Publ. Amsterdam, New York. 377p".

Sanad, S. (1973): "Geology of the area between Wadi El Natrun and El Moghra depression". Ph .D. Thesis, Fac. Sci., Assuit, Univ., Assuit, Egypt, 184 p.

Shata, A. A., (1961): " The geology of groundwater supplies in some arable lands in desert of Egypt " Internal report, Desert Institute, Cairo, Egypt.

Shata, A.A. (1962): "Geology, in: Preliminary report on the geology, hydrology and groundwater hydrology of Wadi El Natrun and adjacent areas". Part. 1, Desert Institute, Cairo, U.A.R; 39 p.

Shata, A.A. and El Fayoumy, I.F. (1967): Geomorphological and morphopedological aspects of the region west of the Nile Delta, with special reference to Wadi El Natrun area. Bull. Inst. Desert d'Egypte, T.XII No. 1, p. 1-38.

Van Der Velpen (1988): "RESIST, Version 1.0, a package for the Processing of the resistivity sounding data" M.Sc. Research Project, ITC, The Netherlands.